Macromolecular Research, Vol. 23, No. 2, pp 177-182 (2015)
DOI 10.1007/s13233-015-3011-7

www.springer.com/13233
pISSN 1598-5032 eISSN 2092-7673

Investigation of the Property Change of Polymer Solar Cells by Changing Counter Anions in Polyviologen as a Cathode Buffer Layer

Thu Trang Do, Hee Seob Hong, Ye Eun Ha, Chan-Young Park, and Joo Hyun Kim*

Department of Polymer Engineering, Pukyong National University, Busan 608-739, Korea

Received August 26, 2014; Revised September 29, 2014; Accepted October 15, 2014

Abstract: Polyviologen (PV) derivatives are known as materials for lowering the work function of cathodes, thereby reducing the electron injection/collection barrier at the cathode interface of polymer solar cells (PSCs). In order to demonstrate the effect of the size of counter anions in PV derivative on the photovolatic properties, we introduce different types of counter anions such as bromide (Br), hexafluorophosphate (PF_6), and *p*-toluene sulfonate (OTs), in PV derivative. The effective work function of the Al electrode is gradually increased by increasing the size of counter anion, indicating the larger counter anion leads to the larger reduction of a Schottky barrier. The power conversion efficiency (PCE) value of the devices is also improved by increasing the size of counter anion. The device (ITO/PEDOT/P3HT:PCBM/PV/Al) with the thin layer of PV derivative bearing a counter anion of OTs as a cathode buffer layer demonstrates the PCE of 3.90%, with a open circuit voltage (V_{oc}) of 0.64 V, a short circuit current density (J_{sc}) of 11.39 mA/cm^2, and a fill factor (FF) of 53.5%, respectively. This is better than the device with PV derivative having a counter anion of PF_6 (PCE=3.73%, J_{sc}=11.14 mA/cm^2, V_{oc}=0.64 V, FF=52.1%) or Br (PCE=3.62%, J_{sc}=10.95 mA/cm^2, V_{oc}=0.64 V, FF=51.6%). Here, our results show that it is possible to improve the performance of PSCs and to tune the electron injection/collection barrier height at the cathode interface by choosing different counter anions without complicated synthesis.

Keywords: polyviologen, buffer layer, anion exchange, polymer solar cell, interface dipole.

Introduction

Many research groups have been focused on polymer solar cells (PSCs) because of the possibility of their application for energy harvesting devices with flexibility and low fabrication cost.[1-3] The electron/hole collection/transporting properties are very important factors for fabrication of the efficient devices, which are strongly related to interfacial properties such as the energy barrier height and adhesive property between the organic semiconducting layer and the anode (or cathode). The properties at the anode interface can be simply improved by insertion of a thin layer of poly(3,4-ethylenedioxylenethiophene):poly(styrenesulfonic acid) (PEDOT:PSS)[4] on ITO, cross-linkable aryl amine derivatives[5-9] on ITO, and self-assembled monolayers (SAMs) modified ITO.[10,11] The active layer can be formed by the solution process without dissolving a pre-coated layer of these materials. As for the cathode interface, the interfacial property is simply improved by insertion of solution processible conjugated polymer electrolytes (CPEs),[12-19] alcohol soluble neutral conjugated polymers,[20,21] polyviologen (PV) derivatives,[22,23] non-conjugated polymer electrolyte (NCPE),[24] and non-conjugated polymers with polar groups, such as polyethylene oxide (PEO),[25] poly(vinyl pyrrolidone) (PVP),[26] and poly(vinyl alcohol) (PVA).[27] These materials enable the fabrication of multilayer device without destroying a pre-coated organic semiconducting layer because of their solubility in polar protic solvents (*e.g.*, water, alcohol, *etc.*). By insertion of the thin layer of these materials at the anode or cathode interface, the performance of devices is dramatically improved relative to the devices without these materials as an interfacial layer.

For CPEs, ionic components of the CPE are accumulated at the top of the CPE surface because the ionic groups are directed away from the hydrophobic semiconducting polymer surface.[28] Thus, ionic groups can help redistribute the electric fields within a device and allow them to show permanent dipoles *via* the spontaneous orientation on the top of either a hydrophobic organic active layer or hydrophilic metal electrode (*i.e.*, cathode). Therefore, it is possible to refine the energy barrier for the electron injection/collection at the cathode interface by the formation of favorable interface dipoles. By placing these ionic groups at the cathode interface, the work function of the cathode can be modified; thus, the energy barrier between the organic semiconducting layer and the cathode can be reduced. In a similar way, the electric fields within a device by the permanent dipoles on the ionic or

*Corresponding Author. E-mail: jkim@pknu.ac.kr

polar groups of the other materials such as NCPE, PEO, PVA, and PVP can be redistributed. Thus, they can refine the energy barrier height at the cathode interfaces by the formation of interface dipoles. Changing the different types of counter anions[29-31] in CPE provides another simple way of tuning the interface properties. Moreover, the work function of the cathode can be simply tuned by the ion density[32] and types of counter anion[33,34] in CPEs.

PV derivatives[22,23] improve the efficiency of either conventional or inverted PSCs by the formation of favorable interface dipoles at the cathode interface, which reduces a Schottky barrier from the active layer to the cathode. In this research, by introducing a different size of counter anion in cationic PV derivative, we investigate the effect of the size of anions on the work function of the cathode and the photovoltaic properties of conventional type PSCs. We refer to PV derivative with bromide (Br), hexafluorophosphate (PF_6) and *p*-toluene sulfonate (OTs) as V-Br, V-PF_6, and V-OTs, respectively. The van der Waals radius of bromide, PF_6, and OTs is 0.19, 0.26, and 0.32 nm, respectively.[35] Generally, the dipole moment (P) of two point charges, one with charge $+q$ and the other with $-q$, is defined as

$$P = q \cdot r$$

where r is displacement vector from the - charge to + charge so that the dipole moment the very thin layer of V-OTs would be bigger than that of V-PF_6 and V-Br. Here, we found that the size of the counter anion affects the electron injection/collection characteristics at the cathode interface of the devices. The PCE values of the device with V-Br, V-PF_6, and V-OTs were 3.62%, 3.73%, and 3.90%, respectively, which are 27.0%, 30.9%, and 36.8% increase compared to that of the device without PV derivatives (2.85%).

Experimental

Materials. Chemicals were purchased from Aldrich Chemical Co. and Alfa Aesar and were used as received unless otherwise described. Regioregular P3HT (Cat. No. 4002-EE) and PCBM (Cat No. nano-cPCBM-BF) were purchased from Rieke Metals Inc. and nano-C, Inc., respectively.

Measurements. The thickness of film was measured by Alpha-Step IQ surface profiler (KLA-Tencor Co.). X-ray photoelectron spectroscopy (XPS, VG Scientific Co.) was recorded using a AlK_α X-ray line (15 kV, 300 W). The work function measurements were carried out using a ultraviolet photoelectron spectroscopy (UPS, VG Scientific Co.) with a He I source ($h\nu$=21.2 eV) at a pressure of 1×10^{-8} Torr. A -3 V was applied to a sample during the measurements to distinguish between the analyzer and sample cut-off. The current density-voltage measurements under 1.0 sun (100 mW/cm^2) condition from a 150 W Xe lamp with an AM 1.5G filter were performed using a KEITHLEY Model 2400 source-measure unit. A calibrated Si reference cell with a KG5 filter certified by National Institute of Advanced Industrial Science and Technology was used to confirm 1.0 sun condition.

Fabrication of Polymer Solar Cells. For fabrication of conventional type PSCs with a structure of ITO/PEDOT/active layer (P3HT:PCBM)/with or without PV/Al, a 40 nm-thick PEDOT:PSS (Baytron P, diluted with 2-propanol, 1:2 v/v) was spin-coated on pre-cleaned indium tin oxide (ITO) glass substrate (sheet resistance=15 ohm/sq). After being baked at 150 °C for 10 min under the air, the active layer was spin-cast from the blend solution of P3HT and PCBM (20 mg of P3HT and 20 mg of PCBM dissolve in 1 mL of *o*-dichlorobenzene (ODCB)) at 600 rpm for 40 s and then dried in covered petri dish for 1 h. The typical thickness of the active layer was 200 nm. Before cathode deposition, cathode buffer layer of a thin layer of PV derivative with different type of counter anion prepared by spin coating with a solution in dimethyl sulfoxide (DMSO) and methanol (MeOH) mixed solvent (DMSO:MeOH=5:95 by volume) onto the active layer. The typical thickness of a cathode buffer layer was less than 5 nm. The Al layer was deposited with a thickness of 100 nm through a shadow mask with a device area of 0.13 cm^2 at 2×10^{-6} Torr. After the cathode deposition, the device was thermally annealed at 150 °C for 10 min in the glove box (N_2 atmosphere).

Synthesis.

Synthesis of Poly(1,1'-didodecyl-4,4'-bipyridinium dibromide) (V-Br): V-Br was synthesized according to the literature procedures.[22,23] A mixture of 4-dibromododecane (0.980 g, 3.00 mmol) and 4,4'-bipyridyl (0.470 g, 3.00 mmol) in 3 mL of *N*,*N*-dimethylformamide (DMF) was stirred at 110 °C for 12 h. The reaction mixture was cooled to room temperature and solid particles in the reaction mixture were collected by filtration and washed with 50 mL of *n*-hexane and 50 mL of dichloromethane. The residues were dried under the vacuum. The yield of yellowish brown solid was 86.8% (1.26 g). ^{1}H NMR (400 MHz, CD_3OD, ppm): δ 9.15-9.12 (Ar-H, 4H), 8.59-8.56 (Ar-H, 4H), 4.77-4.72 (N^+-CH_2-, 4H), 2.15-2.06 (-CH_2-, 4H), 1.42-1.26 (-CH_2-, 16H). ^{13}C NMR (100 MHz, D_2O, ppm): δ 151.12, 146.61, 128.18, 63.46, 31.80, 29.78, 29.67, 29.28, 26.47. Anal. Calcd. for $C_{22}H_{33}Br_2N_2$: C, 54.45; H, 6.85; N, 5.77; Br, 32.93. Found: C, 56.93; H, 7.45; N, 5.31.

Synthesis of Poly(1,1'-didodecyl-4,4'-bipyridinium dihexafluorophosphate) (V-PF_6): V-PF_6 was synthesized by the ion exchange reaction. A solution of 86.0 mg (0.520 mmol) of ammonium hexafluorophosphate in 5 mL of DI water was added dropwise into a solution of a solution of V-Br (61.0 mg, 0.130 mmol) in 5 mL of DI water. The reaction mixture was stirred at room temperature for 24 h. The precipitates were collected by the filtration and washed with copious amount of DI water and dried under the vacuum. The yield was 73.0 mg (89.2%). ^{1}H NMR (400 MHz, DMSO-d_6, ppm): δ 9.37-9.35 (br, 4H), 8.77-8.75 (br, 4H), 4.66 (br, N^+-CH_2-, 4H), 1.97 (br, -CH_2-, 4H), 1.32-1.27 (br, -CH_2-, 16H). Anal. Calcd. For $C_{22}H_{33}F_{12}N_2P_2$:

C, 42.93; H, 5.40; F, 37.04; N, 4.55; P, 10.07. Found: C, 43.15; H, 5.28; 4; N, 4.73.

Synthesis of Poly(1,1'-didodecyl-4,4'-bipyridinium di-*p*-toluenesulfonate) (V-OTs): V-OTs was obtained by the ion exchanged reaction between 61.0 mg (0.130 mmol) of V-Br and 102.0 mg (0.520 mmol) of sodium *p*-toluene sulfonate. The yield was 73.0 mg (89.2%). The yield was 87.0 mg (93.1%). ^{1}H NMR (400 MHz, CD_3OD, ppm): δ 9.23-9.22 (Ar-H, 4H), 8.64-8.62 (Ar-H, 4H), 7.64-7.65 (from OTs, d, J=4.0 Hz, 2H), 7.21~7.19 (from OTs, d, J=4.0 Hz, 2H), 4.72-4.69 (Br, N^+-CH_2-, 4H), 2.34 (from OTs, s, 3H), 2.06 (-CH_2-, 4H), 1.40-1.32 (-CH_2-, 16H). Anal. Calcd. For $C_{36}H_{47}N_2O_6S_2$: C, 64.74; H, 7.09; N, 4.19; O, 14.37; S, 9.60. Found: C, 65.34; H, 7.31; N, 3.99; O, 13.69; S, 9.76.

Results and Discussion

Synthesis and Characterization. As shown in Scheme I, V-OTs was obtained by the simple ion exchange reaction between V-Br solution in deionized (DI) water and a DI water solution with an excess of NaOTs. Then, the precipitates were filtered and washed with a copious amount of DI water until bromide and excess of NaOTs were removed. As shown in Figure 1, the shape of spectra of V-Br and V-PF_6 are very similar to that of V-OTs except the peaks at 7.62-7.54 ppm and 7.16-7.09 ppm, which correspond to the chemical shift of protons in OTs. The number average molecular weight (M_n) of V-Br was 11,243 Da, which is estimated from the relative peak area ratio of the peak at 8.61-8.48 ppm and the peak at 4.22-4.16 ppm, the chemical shift at 8.61-8.48 ppm and 4.22-4.16 ppm correspond to aromatic protons (Ha) on pyridinium ring and methylene protons (Hb) at the end group, respectively. The chemical structures of V-Br, V-PF_6 and V-OTs were also confirmed by a X-ray photoelectron spectroscopy (XPS) (Figure 2). A peak at binding energy of 399 eV was observed, which corresponds to N 1s on pyridinium ring. As shown in Figure 2(a), V-Br showed characteristic peaks of bromide at binding energies of 65.3, 178.5, 185.5, and 252.5 eV,

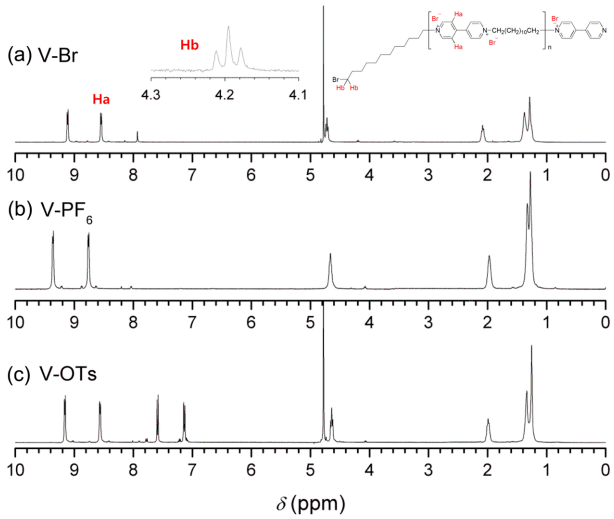

Figure 1. ^{1}H NMR spectrum of (a) V-Br, (b) V-PF_6, and (c) V-OTs.

which correspond to Br 3d, Br 3p3/2, Br 3p1/2, and Br 3s, respectively. The peaks for bromide are completely disappeared in XPS spectra (Figure 2(b) and (c)) of V-PF_6 and V-OTs. The peaks at 684.5 and 29.5 eV in XPS spectrum of V-PF_6 (Figure 2(b)) correspond to F 1s and F 2s. The peaks at binding energies of 230 and 165.5 eV in Figure 2(c) were observed, which correspond to S 2s and S 2p3/2.

Work Function Modification by PV with Different Counter Anion. To understand how the work function of Al is affected by the thin film of V-Br, V-PF_6 and V-OTs, we perform an ultraviolet photoelectron spectroscopy (UPS) experiment, which is well-known instrumentation for investigating the work function and vacuum level shift at the buffer layer/metal interface. It is well known that the work function of metal can be modified by introducing a thin layer of PV derivatives.[22,23] This is due to the formation of a favorable interface dipole at the cathode interface. For measurement of the UPS, a thin film of PV-Xs (X is counter anion) with a thickness of approximately 5 nm was spin-coated from their DMSO/methanol

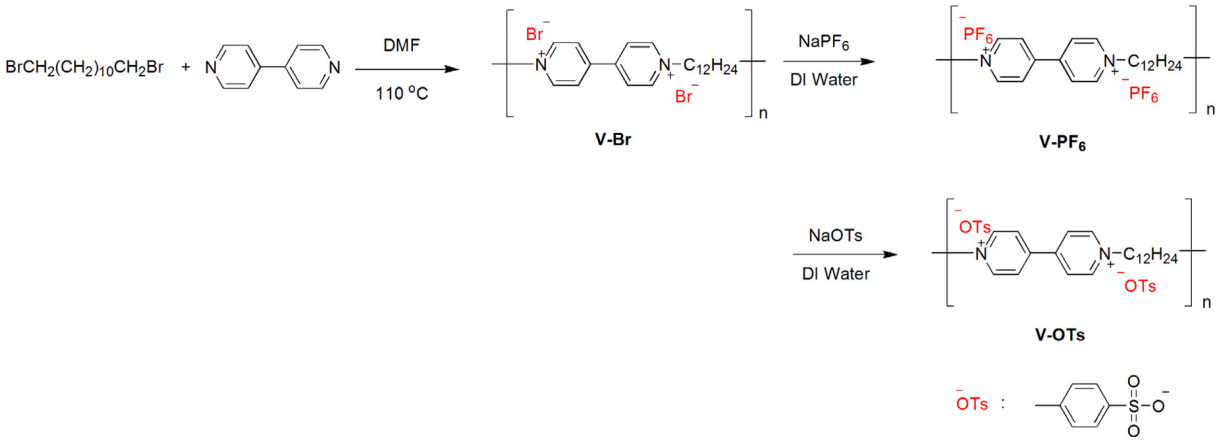

Scheme I. Synthesis of V-Br, V-PF_6, and V-OTs.

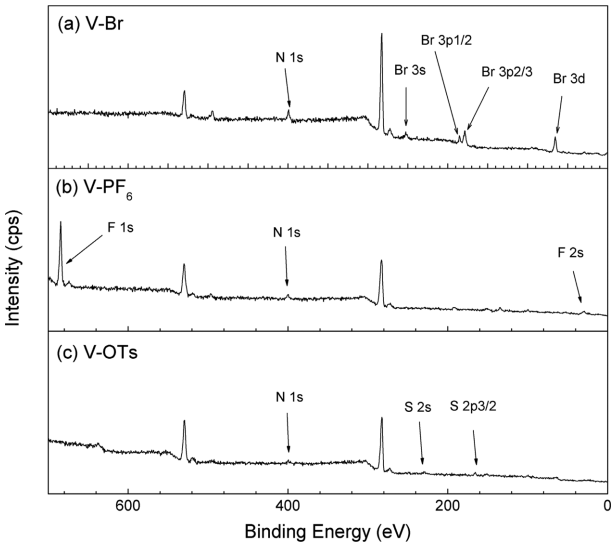

Figure 2. XPS spectra of (a) V-Br, (b) V-PF_6, and (c) V-OTs.

(5/95 by volume) solution on top of a 100 nm-thick Al/glass substrate. As shown in Figure 3(a) and (b), the estimated work function of Al was 4.25 eV, which is estimated from the cut-off energy and the Fermi edge.[22-24,27,36,37] The work function values of V-Br, V-PF_6 and V-OTs coated Al electrode were 4.01, 3.92, and 3.84 eV, respectively, which are smaller than that of Al. Interestingly, a thin layer of PV with larger counter anion leads to a larger reduction of work function (Figure 3(c)). This is presumably due to the size of counter anion. Generally, the dipole moment ionic compound is proportional to the size of the ions, indicating that the magnitude of net dipole moment of PV derivatives are in the order of V-PF_6>V-OTs>V-Br. A larger counter anion on CPEs leads to a larger interface dipole and more pronounced band-bending at the interface between the Au electrode and the thin layer of CPEs, and a smaller effect of work function of the Au cathode.[33] In the very thin film state, layer of PV derivative, ionic components will be directed away from the

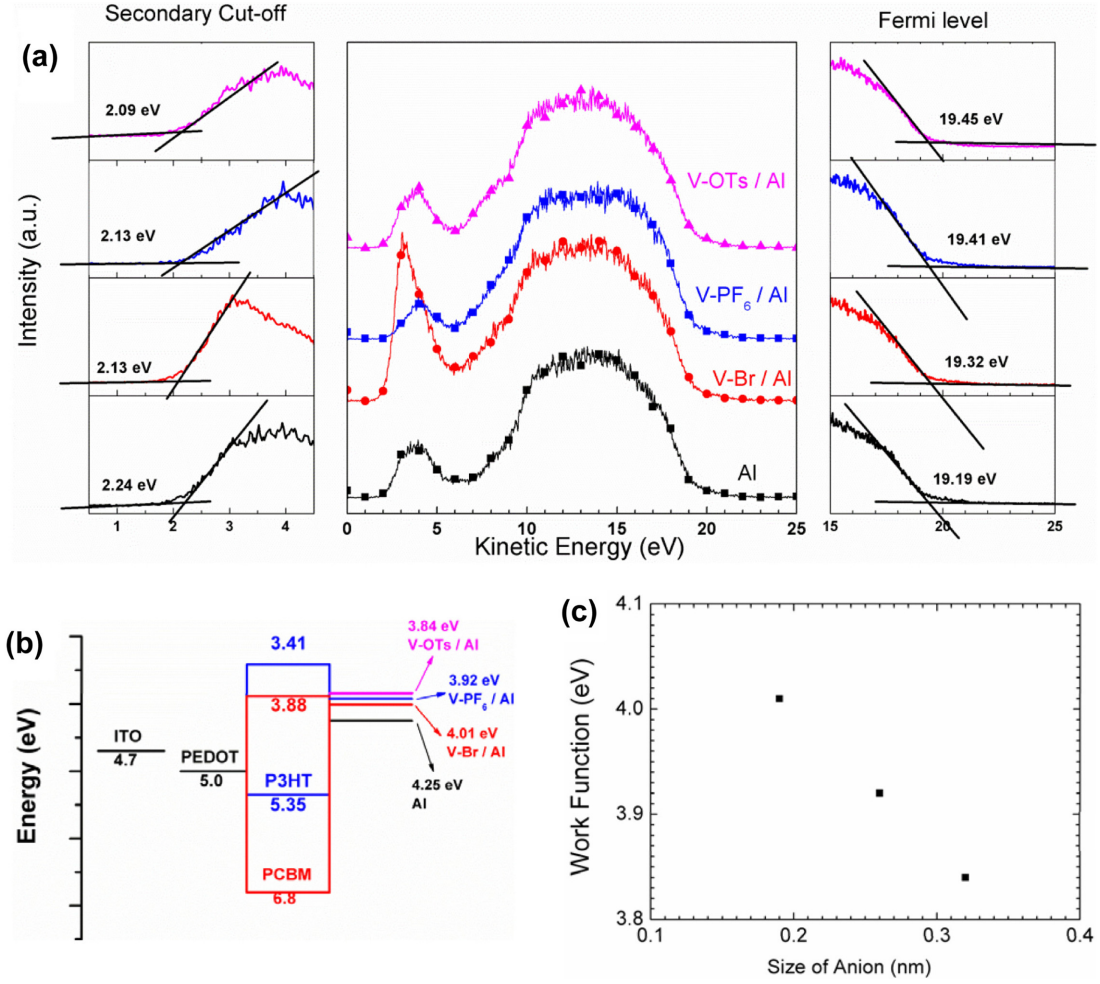

Figure 3. (a) UPS spectrum of a thin layer of V-OTs coated Al, a thin layer of V-PF_6 coated Al, a thin layer of V-Br coated Al, and bare Al electrode, (b) energy level diagram of materials in this research and schematic representation of the work function modification of the cathode by the thin layer of PV derivatives, (c) relationship between the size of counter anion and the effective work function of Al covered PV derivative with applicable counter anion.

surface of the PV layer. This means that the counter anions are directed away from the surface of the PV layer. From our results, one can notice that the reduction of the effective work function of the Al electrode depends on the size of counter anion on PV derivative (as illustrated in Figure 3(b)).

Polymer Solar Cells Using PV with Different Counter Anion. To investigate how the effective work function of Al cathode influences on the photovoltaic properties, we fabricate PSCs having PV derivatives as a cathode buffer layer with a structure of ITO/PEDOT:PSS/active layer (P3HT:PCBM)/PV/Al. A schematic energy diagram of the devices and the work function of the Al electrode with different PV derivatives are shown in Figure 3(b). The V_{oc} values (Figure 4 and Table I) of the devices with PV derivatives were 0.64 V, which is higher than that of the reference device (0.59 V). This is due to the formation of the favorable interface dipoles, which are directed away from the active layer. Here, we found that the V_{oc} enhancement for the device with interlayer was not sensitive to the PV derivatives and the enhancement by the PV derivatives was up to 50 mV. The V_{oc} enhancement may be attributed to the increased built-in potential in the device. As shown in current density-voltage curve under the dark condition (inset of Figure 4(a)), the dark currents of the devices with interlayer were slightly suppressed. This indicates a increase in the

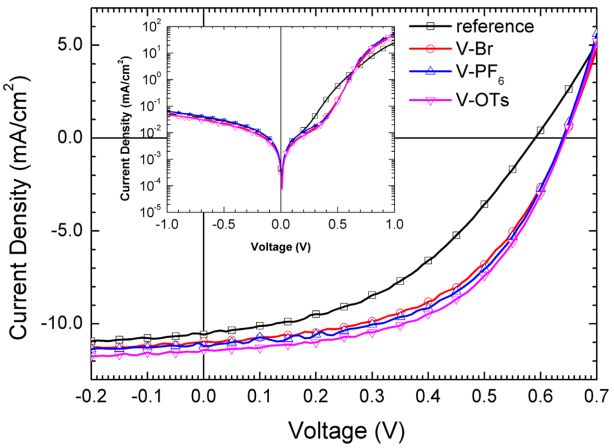

Figure 4. Current density-voltage curves of PSCs under AM 1.5G simulated illumination with an intensity of 100 mW/cm^2 (inset: under the dark condition; □ : reference; ○ : with V-Br; △ : with V-PF$_6$; ▽: with V-OTs).

V_{oc}, which can be understood from the physics of the V_{oc} in p-n junction solar cells.[38] However, the V_{oc} values of the device with PV derivatives seemed not to be affected by the effective WF of the Al electrodes. This is presumably due to a leakage current of the devices with interlayer (inset of Figure 4(a)) were almost the same.

There will be a larger internal electric field in the device than reference device because the energy difference between the work function of the cathode and the work function of the ITO is increased by the formation of favorable interface dipole. Therefore, there is more efficient collection of electrons under the short-circuit condition. This is one plausible reason for the device with PV derivatives showing better performances than the reference device. Thus, as shown in Figure 4 and Table I, the PCEs of the device with V-Br, V-PF$_6$, and V-OTs are 3.62%, 3.73%, and 3.90%, which are dramatically improved over those of the reference device (2.85%). Also, the change of the PCE value exhibits good correlation with the change of the work function of the cathode and the size of counter anion, showing the typical transition from a Schottky to an Ohmic contact. Generally, a large Schottky barrier inhibits the facile injection/collection of electrons at the organic (or polymer) semiconductor/Al interface. Thus, Ohmic contact by the reduction of a Schottky barrier at the interfaces is required to obtain a high J_{sc}.[39,40] Therefore, efficient injecting/collecting of electrons are expected in the device with the V-OTs thin film as a cathode buffer layer.

The series resistance (R_s) of PSCs is an important parameter of PSCs. The R_s was calculated from the inverse slope near the high current regime and the slope near the lower current region in the dark *J-V* curves (inset of Figure 4).[41] By comparing with the reference device (see Table I), the devices with the thin layer of PV derivatives showed smaller R_s and larger FF values, indicating the formation of an Ohmic contact at the cathode interfaces. The R_s values also reflects the contact properties between the active layer and the cathode. Thus, the improved contact property at the cathode interface by the thin layer of PV derivatives is another reason for the improvement of the device performance. As a result, the PSC with the thin layer of V-OTs showed the highest PCE of 3.90%, with a V_{oc} of 0.64 V, a J_{sc} of 11.39 mA/cm^2, and a FF of 53.5%, respectively.

Table I. Summary of Photovoltaic Parameters of PSCs with the Best PCE Value[a]

	V_{oc} (V)	J_{sc} (mA/cm^2)	FF (%)	PCE (%)	R_s (Ω·cm^2)[b]
Reference	0.59 (0.58 ± 0.01)	10.94 (10.66 ± 0.23)	44.2 (43.9 ± 1.22)	2.85 (2.74 ± 0.12)	5.09
V-Br	0.64 (0.64 ± 0.01)	10.95 (10.55 ± 0.25)	51.6 (50.5 ± 1.39)	3.62 (3.41 ± 0.13)	3.06
V-PF$_6$	0.64 (0.64 ± 0.01)	11.14 (11.11 ± 0.03)	52.1 (50.4 ± 1.15)	3.73 (3.59 ± 0.14)	2.72
V-OTs	0.64 (0.64 ± 0.01)	11.39 (10.92 ± 0.37)	53.5 (51.4 ± 1.86)	3.90 (3.61 ± 0.14)	2.86

[a]The averages of photovoltaic parameters for each device are given in parentheses with mean variation. [b]Series (estimated from the device with the best PCE value).

Conclusions

PV derivatives with different counter anoins, such as bromide, PF_6, or OTs have been demonstrated as the cathode buffer layer for PSC to modify the electron injection/collection ability at the cathode interfaces. The increase in the PCE resulted from enhancement of the J_{sc}, the FF, and the V_{oc}, simultaneously. We found that the electron injection/collection barrier was dependent on the size of the counter anion. The larger counter anion leads to a larger reduction of work function. As a result, the performance of PSC with V-OTs showed the PCE of 3.90%. This research provides a very simple and facile strategy compared with the structural refinement by complicated synthesis.

Acknowledgments. This research was supported by Converging Research Center Program through the Ministry of Education, Science, and Technology (2013K000196), and the Basic Science Research Program through the National Research Foundation of Korea (NRF) funded by the Ministry of Education, Science, and Technology (2014055822).

References

(1) G. Yu, J. Gao, J. C. Hummelen, F. Wudl, and A. J. Heeger, *Science*, **270**, 1789 (1995).
(2) W. U. Huynh, J. J. Dittmer, and A. P. Alivisatos, *Science*, **295**, 2425 (2002).
(3) S. Gunes, H. Neugebauer, and N. S. Sariciftci, *Chem. Rev.*, **107**, 1324 (2007).
(4) F. L. Zhang, M. Johansson, M. R. Andersson, J. C. Hummelen, and O. Inganas, *Adv. Mater.*, **14**, 662 (2002).
(5) E. Bacher, M. Bayerl, P. Rudati, N. Reckefuss, C. D. Muller, K. Meerholz, and O. Nuyken, *Macromolecules*, **38**, 1640 (2005).
(6) H. Hong, M. Y. Jo, Y. E. Ha, and J. H. Kim, *Macromol. Res.* **21**, 321 (2013).
(7) S. Liu, X. Jiang, H. Ma, M. S. Liu, and A. K. Y. Jen, *Macromolecules*, **33**, 3514 (2000).
(8) M. S. Liu, Y. H. Niu, J. W. Ka, H. L. Yip, F. Huang, J. Luo, T. D. Kim, and A. K. Y. Jen, *Macromolecules*, **41**, 9570 (2008).
(9) Y. Lim, Y. S. Park, Y. Kang, D. Y. Jang, J. H. Kim, J.-J. Kim, A. Sellinger, and D. Y. Yoon, *J. Am. Chem. Soc.*, **133**, 1375 (2011).
(10) S. Khodabakhsh, B. M. Sanderson, J. Nelson, and T. S. Jones, *Adv. Funct. Mater.*, **16**, 95 (2006).
(11) C. Goh, S. R. Scully, and M. D. McGehee, *J. Appl. Phys.*, **101**, 114503 (2007).
(12) H. Choi, J. S. Park, E. Jeong, G. W. Kim, B. R. Lee, S. O. Kim, M. H. Song, H. Y. Woo, and J. Y. Kim, *Adv. Mater.*, **23**, 2759 (2011).
(13) S. H. Oh, S. I. Na, J. Jo, B. Lim, D. Vak, and D. Y. Kim, *Adv. Funct. Mater.*, **20**, 1977 (2010).
(14) W. Ma, P. K. Iyer, X. Gong, B. Kiu, D. Moses, G. C. Bazan, and A. J. Heeger, *Adv. Mater.*, **17**, 274 (2005).
(15) S. I. Na, S. H. Oh, S. S. Kim, and D. Y. Kim, *Org. Electron.*, **10**, 496 (2009).
(16) Y. Jin, G. C. Bazan, A. J. Heeger, J. Y. Kim, and K. Lee, *Appl. Phys. Lett.*, **93**, 123304 (2008).
(17) X. Zhu, Y. Xie, X. Li, X. Qiao, L. Wang, and G. Tu, *J. Mater. Chem.*, **22**, 15490 (2012).
(18) J. Fang, B. H. Wallikewitz, F. Gao, G. Tu, C. Muller, G. Pace, R. H. Friend, and W. T. S. Huck, *J. Am. Chem. Soc.*, **133**, 683 (2011).
(19) C. Min, C. Shi, W. Zhang, T. Jiu, J. Chen, D. Ma, and J. Fang, *Angew. Chem. Int. Ed.*, **52**, 3417 (2013).
(20) F. Huang, Y. Zhang, M. S. Liu, and A. K. Y. Jen, *Adv. Funct. Mater.*, **19**, 2457 (2009).
(21) H. Wu, F. Huang, Y. Mo, W. Yang, D. Wang, J. Peng, and Y. Cao, *Adv. Mater.*, **16**, 1826 (2004).
(22) M. Y. Jo, Y. E. Ha, and J. H. Kim, *Sol. Energy Mater. Sol. Cells*, **107**, 1 (2012).
(23) M. Y. Jo, Y. E. Ha, and J. H. Kim, *Org. Electron.*, **14**, 995 (2013).
(24) G. E. Lim, Y. E. Ha, M. Y. Jo, J. Park, Y. -C. Kang, and J. H. Kim, *ACS Appl. Mater. Interfaces*, **5**, 6508 (2013).
(25) F. Zhang, M. Ceder, and O. Inganas, *Adv. Mater.*, **19**, 1835 (2007).
(26) H. Wang, W. Zhang, C. Xu, X. Bi, B. Chen, and S. Yang, *ACS Appl. Mater. Interfaces*, **5**, 26 (2013).
(27) Y. E. Ha, G. E. Lim, M. Y. Jo, J. Park, Y. C. Kang, S. J. Moon, and J. H. Kim, *J. Mater. Chem. C*, **2**, 3820 (2014).
(28) J. Park, R. Yang, C. V. Hoven, A. Garcia, D. A. Fischer, T. Q. Nguyen, G. C. Bazan, and D. M. DeLongchamp, *Adv. Mater.*, **20**, 2491 (2008).
(29) J. H. Seo, R. Yang, J. Z. Brzezinski, B. Walker, G. C. Bazan, and T. Q. Nguyen, *Adv. Mater.*, **21**, 1006 (2009).
(30) J. H. Seo and T. Q. Nguyen, *J. Am. Chem. Soc.*, **130**, 10042 (2008).
(31) Y. M. Chang, R. Zhu, E. Richard, C. C. Chen, G. Li, and Y. Yang, *Adv. Funct. Mater.*, **22**, 3284 (2012).
(32) B. H. Lee, I. H. Jung, H. Y. Woo, H. K. Shim, G. Kim, and K. Lee, *Adv. Funct. Mater.*, **24**, 1100 (2014).
(33) J. H. Seo, Y. Jin, J. Z. Brzezinski, B. Walker, and T. Q. Nguyen, *ChemPhysChem*, **10**, 1023 (2009).
(34) J. H. Seo, R. Yang, J. Z. Brzezinski, B. Walker, G. C. Bazan, and T. Q. Nguyen, *Adv. Mater.*, **21**, 1006 (2009).
(35) Informations are taken from http://www.chemspider.com and ttp://www.chemicalize.org.
(36) S. I. Na, T. S. Kim, S. H. Oh, J. Kim, S. S. Kim, and D. Y. Kim, *Appl. Phys. Lett.*, **97**, 223305 (2010).
(37) Y. Park, V. Choong, Y. Gao, B. R. Hsieh, and C. W. Tang, *Appl. Phys. Lett.*, **68**, 2699 (1996).
(38) P. W. M. Blom, V. D. Mihailetchi, L. J. A. Koster, and D. E. Markov, *Adv. Mater.*, **19**, 1551 (2007).
(39) (a) S. M. Sze, in *Physics of Semiconductor Devices,* Wiley-Interscience, New York, 2nd ed., 1981, p 222. (b) C. Waldauf, M. C. Scharber, P. Schilinsky, J. A. Hauch, and C. J. Brabec, *J. Appl. Phys.*, **99**, 104503 (2006). (c) C. He, C. Zhong, H. Wu, R. Yang, W. Tang, F. Huang, G. C. Bazan, and Y. Cao, *J. Mater. Chem.*, **20**, 2617 (2010).
(40) H. L. Yip, S. K. Hau, N. S. Baek, H. Ma, and A. K. Y. Jen, *Adv. Mater.*, **20**, 2376 (2008).
(41) J. Xue, S. Uchida, B. P. Rand, and S. R. Forrest, *Appl. Phys. Lett.*, **84**, 3013 (2004).